MSDE

PAPER

View Article Online
View Journal | View Issue

Open Access Article. Published on 04 November 2025. Downloaded on 1/20/2026 7:39:08 PM.
This article is licensed under a Creative Commons Attribution 3.0 Unported Licence.

Check for updates

Cite this: *Mol. Syst. Des. Eng.*, 2026, **11**, 126

Simulation of the microalgae-enriched nitrogen fertilizer granulation mechanism using the DEM method

Rasa Šlinkšienė, *[a] Vaidas Bivainis[b] and Austėja Mikolaitienė[a]

Received 3rd June 2025,
Accepted 21st October 2025

DOI: 10.1039/d5me00091b

rsc.li/molecular-engineering

The use of granular fertilizers offers significant advantages over traditional powder forms, including improved nutrient distribution, reduced dust, and controlled nutrient release. These benefits enhance plant growth while minimizing negative environmental impacts. The addition of reused materials (recycle) significantly influences the size distribution and strength of granular fertilizers. It was determined that incorporating 60% recycle increases the part of commercial granules (size 2.0–4.0 mm) from 22% to about 68%. However, this increase is accompanied by a decrease in static strength, which drops from 2.8–3.8 MPa to 1.7–2.3 MPa. Modelling granulation processes holds substantial potential for the fertilizer industry, enabling the optimization of high-quality granular fertilizer production while minimizing the need for extensive experimental trials. This approach not only streamlines manufacturing but also ensures consistent nutrient supply, ultimately contributing to improved crop yields and sustainable agricultural practices. In this study, a simulation model based on an actual granulation drum was used to investigate the granulation process of a mixture containing recycled material, crystalline urea, and the microalgae *Chlorella vulgaris* sp. The granulation simulation data showed that granule formation began within 30 seconds and that the desired quantity of the mixture was produced in just 30 seconds. Throughout the process, the segregation coefficient remained near zero, indicating effective granule formation and distribution.

Design, System, Application

The granulation process optimization strategy presented in this work, combining experimental studies and molecular modelling, allows for effective control of granule formation, their size distribution, and mechanical properties of the mixture. Modelling, based on the simulation of a real granulation drum, makes it possible to reduce the need for physical experiments and accelerate the search for technological solutions. The study revealed that the amount of return in the mixture significantly affects both the granule size fractions and their strength, which allows for targeted adjustment of product quality according to the desired functionality. Design constraints, such as material interactions, particle size distribution, and the effect of the binder, were systematically evaluated both through modelling and experimentation. The results of the study have significant application potential in sustainable agricultural production – using microalgae, it is possible to regulate urea solubility and reduce environmental pollution. The proposed approach can also be applied to other systems where the aim is to combine recycled materials and environmentally friendly raw materials.

1. Introduction

Most industries (food, pharmaceutical, fertilizer, construction) use granular materials, but the size and properties of granules vary. Granular fertilizers have many advantages compared to powdered or crystalline fertilizers. First, they are less dusty, and due to their appropriate size and spherical shape, they are easier to spread by hand or with specialized fertilizer spreading machines, thus ensuring an even distribution of nutrients. Granular fertilizers also enable a slower, long-term release of nutrients, which benefits plants by ensuring a stable supply of nutrients over time. For the same reason, they are less likely to be washed away by rain or dissolved by atmospheric moisture. Additionally, granules are less prone to absorbing moisture and clumping together, making them easier to store and transport.[1,2] In general, granular fertilizers are more convenient to use, more efficient in terms of nutrient distribution, and less harmful to the environment and health compared to powdered forms.

However, some granular fertilizers, such as urea, dissolve quickly regardless of their form. Because urea is widely used

[a] Department of Physical and Inorganic Chemistry, Kaunas University of Technology, Radvilenu St. 19, LT-50270 Kaunas, Lithuania.
E-mail: rasa.slinksiene@ktu.lt
[b] Department of Agricultural Engineering and Safety, Faculty of Engineering, Agriculture Academy, Vytautas Magnus University, Studentu Str. 15A, LT-53362 Akademija, Kaunas District, Lithuania

This journal is © The Royal Society of Chemistry and IChemE 2026

Open Access Article. Published on 04 November 2025. Downloaded on 1/20/2026 7:39:08 PM.
This article is licensed under a Creative Commons Attribution 3.0 Unported Licence.

in crops and is highly soluble, it causes significant losses due to volatilization and leaching. These losses reduce nitrogen use efficiency in plants, limit crop yields, and contribute to environmental pollution, including hazardous gas emissions and water eutrophication.[3] Coating physical urea pellets with a suitable material is one method of producing controlled-release urea. This urea coating technology not only reduces nitrogen losses caused by volatilization and leaching but also modifies the kinetics of nitrogen release. This, in turn, ensures that nutrients are supplied to plants at a rate more aligned with their metabolic needs.[4] The controlled release of nutrients also depends on ambient temperature and humidity, with release rates increasing at higher temperatures and humidity levels.[5]

The solubility of nitrogen compounds in water can be reduced by physical methods, such as coating or encapsulating substances with organic or inorganic materials, and by chemical methods, such as converting nitrogen into less soluble polymeric forms. Fertilizer granules are typically coated with low-water-soluble materials, which allows water to slowly penetrate and dissolve the nutrients over time, leading to prolonged nutrient release.[3,6–9] Another option for slowing down the solubility of nitrogen fertilizers is to use organic or biofertilizers, which enrich the soil with nutrients without deteriorating soil quality.[10,11]

One suitable bioactive material is algae, which are described as a group of mostly aquatic, photosynthetic organisms that lack the roots, stems, leaves, and complex reproductive structures of true plants. They possess diverse photosynthetic pigments and unique cellular properties not found in plants or animals. While most algae photosynthesize to produce their own food from sunlight and carbon dioxide, there are certain species of algae that require only external sources for nutrition.[12,13] Algae have diverse commercial uses, including as food and beverage ingredients, biofuels, biomedicine, cosmetics, fertilizers, and pigments.[14–18] They are particularly valuable for bioenergy and biofuel production, as well as for their positive effects on crop yields when used as fertilizers. Algae cultivation helps reduce atmospheric CO_2, contributing to climate change mitigation.[19–25] Unlike traditional crops, algae do not require agricultural land and can be grown in environmentally friendly, closed cycles. Studies show that microalgal biomass provides a slow release of nutrients, enhancing plant growth and resilience.[26–28] Thus, after careful analysis and evaluation of the chemical composition, this biomass can be used in the production of "green" fertilizers, and the use of seaweed microalgae for these purposes is quite extensive.[29] Studies by Mulbry *et al.*[30,31] show that pure microalgal biomass is characterized by the slow release of nitrogen, phosphorus, and potassium, meeting plant needs. With high concentration of nitrogen and enriched with biosolids, such granular fertilizers release nutrients slowly and are, therefore, regarded as advanced and have great future prospects.

High-quality granulation of fertilizers largely depends on their composition and technological parameters.[32,33] The agglomeration process has a particularly strong influence on product quality, analysis of which in high-performance devices is problematic. Therefore, it is very important to be able to predict and describe the course of the process of agglomeration using mathematical modelling. Considering the challenges described, the aim of this work was to create a model of the wet granulation process for a mixture of a crystalline urea and microalgae based on experimental data.

This study shows that the discrete element method (DEM) can simulate the wet granulation of a microalgae-enriched nitrogen fertilizer mixture, with simulation results validated against laboratory experiments in a drum granulator. The new contribution of this work is the development of a predictive DEM model that represents key stages of the granulation process – including mixing dynamics and granule formation—thus enabling more efficient design and optimization of fertilizer production processes.

2. Materials and methods

2.1. Granulation of fertilizers

The raw materials for producing granulated bioactive nitrogen fertilizers were crystalline urea (CU) p.a., "Reachem", Slovakia, and *Microalgae Chlorella vulgaris* sp. (MAChV), obtained from Buxtrade GmbH, Germany. Water (W) was used as a binder. In this research, the laboratory drum granulator used is a prototype of the granulator employed in the production of commercial bulk fertilizers. The ratios of the length, width, and other geometrical parameters of the drum granulator are directly proportional to that of the commercial one. The laboratory drum granulator is a reduced-size version of the industrial granulator. The model of the granulator is shown in Fig. 1. A mixture of raw materials was prepared for granulation and moistened with water before the process. The mixture consisted of 80%, 60%, and 40% bulk materials (CU : MAChV ratio 9 : 1) and 20%, 40%, and 60% recycled materials (R) with the same composition as the bulk materials. The recycled material consists of improperly sized granules (less than 2 mm) obtained by granulating urea with microalgae and water. The granulation process was carried out under the following

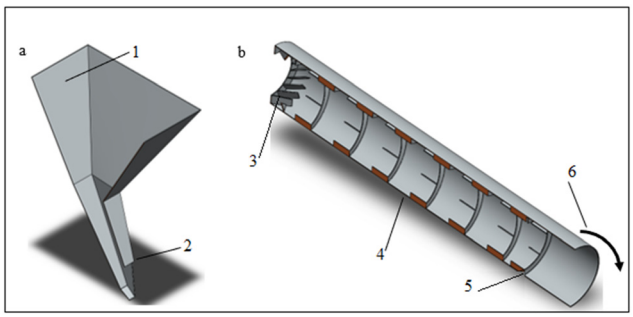

Fig. 1 Sectional views of a) hopper and b) drum granulator. 1 – location of "particle factory", 2 – hopper inlet, 3 – mixture distribution section, 4 – granulation section, 5 – discharging section, 6 – granulator rotation.

Open Access Article. Published on 04 November 2025. Downloaded on 1/20/2026 7:39:08 PM.
This article is licensed under a Creative Commons Attribution 3.0 Unported Licence.

conditions: drum tilt angle was 3°, rotation speed was 26 rpm, operating temperature ranged 58.1 ± 1.4–62.1 ± 2.0 °C, and granulation cycle time was 5–6 minutes. This temperature range was chosen based on the thermal stability of the raw materials and to prevent urea decomposition. The selection of the aforementioned granulation parameters was based on an extensive experimental investigation by the authors. These specific conditions were determined to be optimal for achieving the desired granule morphology, size distribution, and mechanical strength, along with other essential properties critical for product quality and performance. The aim of the simulation was to create and validate a model of the process of granulation using a laboratory granulator model and a set of experimentally confirmed granulation parameters.

2.2. Determining properties of granular nitrogen fertilizers

Particle size distribution based on diameter was determined using RETSCH (Retsch GmbH, Haan, Germany) woven wire sieves with aperture sizes ranging from 0.2 mm to 7.0 mm. Each fraction of granules with different diameters was collected, weighed, and expressed as a percentage by mass.

According to the ISO 10390:2005 standard, to measure the pH values of the granular product, granules were dissolved in water (10 wt% concentration solution) and filtered. Furthermore, each test sample was prepared in duplicate, and a Whatman grade 589/3, blue ribbon filter was used to filter the obtained suspensions. Following this, the pH values were determined using a HANNA instruments pH 211 microprocessor (HANNA Instruments, Woonsocket, USA) pH meter.[34]

Granules of commercial fraction with diameters of 2.0–3.15 mm and 3.15–4.0 mm were used for the crushing strength measurements. It is crucial to obtain the appropriate granule strength to maintain its shape and form throughout all handling procedures (from various manufacturing stages to application). To perform this study, at least 20 granules of similar size and shape were selected from each fraction. The crushing strength is defined as the amount of compression force applied to the granule until the first crack appears.[35] The crushing strength test was carried out using an IPG-2 (АО "УНИХИМ с ОЗ", Yekaterinburg, Russia) device. The compressive force was measured in N, but the results are expressed in MPa.

The loose bulk density was determined according to the gravimetric method by pouring the material into a graduated cylinder of a known volume, as described in the ISO 7837:2001 standard.[36] To determine the density, the empty cylinder was first weighed, followed by the cylinder containing the granules. The calculated mass difference corresponds to the mass of freely poured material per unit volume. Each measurement was repeated twice.

The moisture content of the granular product (2–4 mm size) was determined using an electronic moisture analyser KERN MLS 50-3HA160N (KERN & Sohn GmbH, Balingen, Germany). The drying program applies a uniform temperature increase up to 60 °C, and the moisture content result is given as a percentage. The measurements were repeated three times to ensure the reliability of the results.

A Dino-Lite Premiere digital microscope (AnMo Electronics Corporation, Taipei, Taiwan) was used to obtain optical images of the raw material particles and granules at 200× and 60× magnification. The microscope software allows the measurement of objects and displays the dimensions in the captured images.

2.3. Modelling and material properties of the drum granulator

The computer models of the feeder and drum granulator used in the modelling studies were created using SolidWorks 2024 EDU software. The models of the feeder and drum granulator are shown in Fig. 1, and their main geometric parameters are provided in Table 1.

The granulator consists of three main parts: the mixture distribution section, the granulation section, and the granule discharging section. The materials from the granulator's mixture distribution section were fed into the granulation section, where they were mixed and granulated by the spiral and tangential impellers. At the end of the drum granulator, granules and the residual material mixture pass through the inner ring and enter the granule discharge section. The raw material for granulation was supplied through a hopper placed in the first mixture distribution section of the drum granulator. The rotation speed of the granulator was 26 rpm, and the angle of inclination of the drum was 3°. The hopper and the drum were made of 1 mm thick AISI 304 stainless steels. The main characteristics of the material[37] are presented in Table 2.

The key boundary conditions, including the feeder, drum geometry, tilt angle, inlet and outlet, and wall properties, were derived from our experimental studies on urea–microalgae granulation. Optimal parameters were identified by varying the tilt angle (2–5°), rotation speed (22–28 rpm), and residence time (5–10 min) according to granule formation quality. These conditions were then applied not

Table 1 Geometry of the feeder and drum granulator

Parameters	Value
Volume of the granulator, L	4.17
Length of granulator, mm	570
Outer/inner diameter, mm	100/98
Inclination angle, °	3
Mixture distribution section length, mm	41
Granulation section length, mm	439
Granulation discharging section length, mm	90
Granulation spiral pitch, mm	73
Granulation spiral, inner rings and granulation blades' height, mm	9
Hopper inlet height × width, mm	59 × 33
Distance of the inlet from the mixing blades and from the start of the granulator, mm	10
Equipment material thickness, mm	1

 This journal is © The Royal Society of Chemistry and IChemE 2026

Open Access Article. Published on 04 November 2025. Downloaded on 1/20/2026 7:39:08 PM.
This article is licensed under a Creative Commons Attribution 3.0 Unported Licence.

Table 2 Material properties of equipment

Properties	Density, kg m^{-3}	Young's modulus, MPa	Poisson's ratio
Value	8000	190 000	0.29

only in this study but also in other works on fertilizer granulation.[38–42]

2.4. Discrete element modelling (DEM) of the granulation process

Granulation of the particle mixture was simulated using the Altair EDEM 2023 discrete element modelling software. Initially, the required particle flow was generated. The initial flow rate of the supplied particles was simulated for 25 seconds, during which 50 g of the mixture was generated. The initial flow of the bulk material particles was generated by a software particle factory. This virtual factory introduced particles into the simulation at a controlled generation rate, position, and orientation, mimicking a laboratory feed as realistically as possible. The virtual factory shape was a rectangular parallelepiped that was placed in the upper part of the hopper (Fig. 1 and 7(a)); this placement closely simulated the mixture feeding during the experiment. To verify the proper generation of particle mass, a virtual total mass sensor was placed under the hopper inlet, and the total mass of the generated particles is presented in Fig. 4. After generating the required amount of particles, the granulation process continued for about 7 minutes. More details about the DEM simulation parameters are given in sections 3.2 and 3.3.

In the granulation modelling studies, the binder (water) used was evaluated by modifying the mixture properties, *i.e.*, the mixture properties were altered so that the properties of the mixture of particles in the final model were close to the properties of the real experimental mixture. During the modelling studies, all the selected particle properties were calibrated. The calibration of the particles' properties and the discrete element model was primarily achieved through visual comparisons with experimental observations. A visual comparison of the modelling and experimental studies was essential for validation because no intermediate parameters of the granulation process were recorded during the physical experiments. This approach was crucial for assessing process dynamics that could not be captured by real-time measurements. Furthermore, visual comparison is often a fundamental validation approach in the simulation of complex systems and processes, particularly when a lack of intermediate experimental data precludes quantitative comparison.

The first stage of verification involved ensuring that the simulated particle flow through the hopper inlet was consistent with experimental behaviour. Fig. 7(a) shows a snapshot of the simulated particle flow from the virtual particle factory to the hopper inlet. Throughout the simulation, the particle mixture exhibited a stable and uniform flow, with no visible sticking to the hopper walls. This behaviour was also confirmed by direct observations during the laboratory experiments. Furthermore, the granulation dynamics of the particle mixture within the drum granulator, including particle–particle and particle–wall interactions such as sticking and discharging, were validated through visual comparison with experimental footage. The results of this visual comparison are presented in Fig. 7(c and d). Based on this, it can be stated that this visual agreement confirmed the selection of appropriate particle–particle and particle–wall properties for the model. Observation of seeded granule formation, where fine particles were seen adhering to larger ones, further validated the choice of simulation parameters.

2.5. Statistical analysis

All measurements of the fertilizer physical properties were performed in triplicate, with 6 or 20 replicates, depending on the parameter analysed. The data are expressed as mean ± standard deviation (SD). For each sample, the static crushing strength was measured on 20 granules (n = 20), while other physicochemical properties (*e.g.*, moisture content, pH, electrical conductivity, nutrient content) were determined in triplicate (n = 3). Experimental particle size was determined on 6 granules (n = 6) using a digital microscope. Statistical differences among treatments were evaluated by one-way analysis of variance (ANOVA) at a significance level of $p < 0.05$. All statistical analyses were performed using Microsoft Excel 2021 (Microsoft Corp., USA).

3. Results and discussion

3.1. Properties of granular nitrogen fertilizers

Urea, microalgae, and a recycle of the same composition formed during previous granulation processes, as described in our earlier study,[38] were used to investigate the influence of recycling on the properties of granules. The resulting granulated product was dried in a laboratory dryer until it

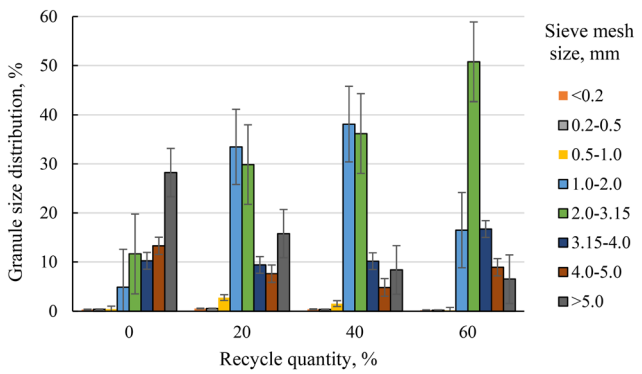

Fig. 2 Granule size distribution of microalgae-enriched nitrogen fertilizers in relation to the amount of recycle. Values represent mean ± standard deviation (n = 3). Statistical differences among treatments were evaluated by one-way ANOVA at a significance level of $p < 0.05$.

Open Access Article. Published on 04 November 2025. Downloaded on 1/20/2026 7:39:08 PM.
This article is licensed under a Creative Commons Attribution 3.0 Unported Licence.

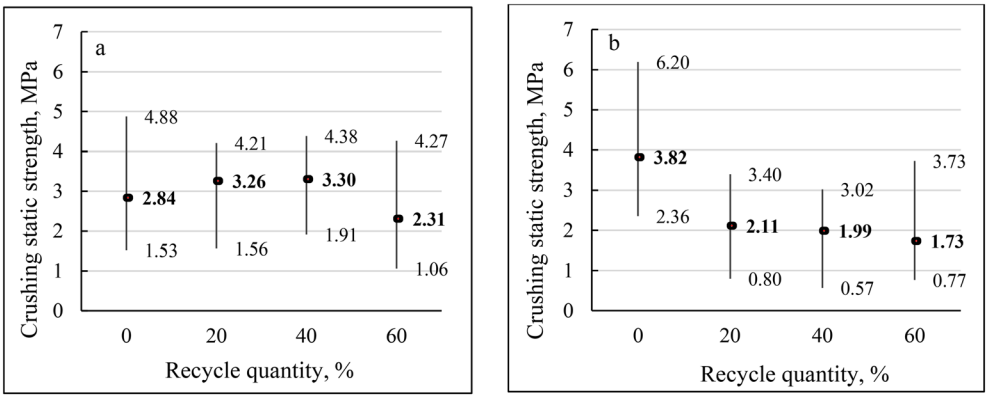

Fig. 3 Crushing static strength of microalgae-enriched nitrogen fertilizer granules depending on the amount of recycle: a) 2.0–3.15 mm granules, b) 3.15–4.0 mm granules. Values represent mean ± standard deviation (n = 20). Statistical differences among treatments were evaluated by one-way ANOVA at a significance level of $p < 0.05$.

reached a stable mass, after which its properties were evaluated. The most important properties of granular fertilizers, granulometric composition and strength, are presented in Fig. 2 and 3.

The results in Fig. 2 show that the addition of recycle significantly affects the size distribution of granules. When 20% and 40% recycle is added to the raw material mixture, the amount of 1.0–2.0 mm and 2.0–3.15 mm granules increase by more than threefold compared to granulation without recycle. Further increasing the recycling rate to 60% alters the particle size distribution with 2.0–3.15 mm granules constituting about 50% of the product. Woodroof emphasizes that the specifications of fertilizers regarding the particle size distribution impose stringent requirements on manufacturers. Generally, granules are expected to range from 1.0 to 5.0 mm in size, with over 90% falling between 2.0 and 4.0 mm.[43] However, at this stage, the results achieved under laboratory conditions do not fully meet these standards. It is anticipated that optimizing the process conditions across a wider range could yield improved granule size distribution results,[44] but this would require an enormous amount of physical investigation.

We hypothesize that such experimental studies could be significantly enhanced by the development of a granulation model. This would represent a major advancement in optimizing industrial plant operations and improving the quality of granular fertilizers. A uniform particle size ensures even distribution of granules in the field, while optimally shaped granules contribute to efficient and controlled nitrogen leaching into the soil.[43]

Research shows that different granulation technologies, such as accretion and agglomeration methods, influence granule strength. Granules produced by accretion are generally stronger and more durable than agglomerated ones, resulting in less damage during transport and reduced risk of dust generation.[45] The type of granulator thus affects various granule parameters, including their resistance to crushing and other mechanical effects. The simplest plate granulators for solid bulk fertilizers[44,46] have low productivity, and the process is difficult to control due to the interaction between the granulation pan and the environment. A significantly more advanced and technologically capable device is the drum granulator. Granules produced by accretion reach a compressive strength of about 4–8 kg,[45] which, for an average 3 mm pellet, corresponds to 5.55–11.10 MPa when converted from kg to MPa. As shown in Fig. 3, the granules obtained during wet granulation in our laboratory conditions exhibit lower static strength on average, which varies depending on the granule size: 2.31–3.30 MPa for granules of size 2.0–3.15 mm and 1.73–3.82 MPa for granules of size 3.15–4.0 mm.

Both granule fractions (2.0–3.15 mm and 3.15–4.0 mm) show a clear trend – with an increasing amount of recycle, the strength of the granules decreases. Smaller granules (2.0–3.15 mm) exhibit slightly higher strength than larger granules (3.15–4.0 mm), especially at lower recycle quantities. For example, without recycle the static strength is about 2.84 MPa (Fig. 3a) and 3.82 MPa (Fig. 3b), but at 60% recycle it decreases to 2.31 and 1.73 MPa, respectively. Large dispersion intervals (especially without recycle) indicate that the strength of the granules is quite uneven, which is likely due to the varying properties of the raw materials and their uneven distribution at the initial mixing stage. In general, the decrease in the static strength of the granules indicates that recycle negatively affects the adhesion and mechanical integrity of the urea granules enriched with microalgae. The raw material mixture containing recycle represents a system into which already dried, harder particles with lower plasticity are introduced. It is known that stronger interaction forces occur between particles of similar size, whereas the interaction between smaller raw material particles and larger recycle particles is weaker, which in turn influences the granule formation mechanism. Our results agree with the research of Macák *et al.*, who found that smaller fertilizer particles and a more uniform granulometric structure increase granule resistance to pressure, reducing the risk of breakage.[47]

 This journal is © The Royal Society of Chemistry and IChemE 2026

Open Access Article. Published on 04 November 2025. Downloaded on 1/20/2026 7:39:08 PM.
This article is licensed under a Creative Commons Attribution 3.0 Unported Licence.

Table 3 Physical characteristics of the raw materials' mixture and microalgae-enriched nitrogen fertilizer granules. Values represent mean ± standard deviation (n = 3 or n = 20)

Raw materials' mixture			Granular fertilizers			
Ratio CU : MAChV	Recycle quantity, %	Raw materials' moisture, %	Commercial fraction (2.0–4.0 mm) quantity, %	Granule moisture, %	Bulk density, kg m^{-3}	pH of 10% fertilizer solution
9 : 1	0	13.42 ± 0.02	21.89 ± 2.58	1.0 ± 0.04	392.0 ± 2.48	5.9
9 : 1	20	13.74 ± 0.02	39.24 ± 0.15	1.1 ± 0.04	432.1 ± 1.18	5.9
9 : 1	40	14.44 ± 0.01	46.32 ± 0.10	1.0 ± 0.05	430.4 ± 1.31	5.9
9 : 1	60	15.13 ± 0.02	67.49 ± 0.07	1.1 ± 0.06	457.4 ± 0.80	6.0

Other properties, such as moisture, bulk density, pH of granular fertilizers, are presented in Table 3.

The amount of moisture used to wet the raw materials directly depends on the amount of recycle used. It is evident that the amount of the marketable fraction (2–4 mm) is significantly higher when recycle is applied. It was found that the bulk density increases with the use of recycle, while the moisture content of the final product remains unchanged.

3.2. Geometry and material properties of the particles

The microscopic model for discrete element modelling is defined by three key parameter sets: particle properties, interaction parameters, and the contact adhesion model. Particle properties specifically encompass particle shape, material density, Young's modulus, and Poisson's ratio.

The shape, size, and mass fraction of the particles in the mixture, as well as the material properties of the used particle materials, and the flow rate and mass of each part of the mixture during the initial 25 seconds of the study are given in Table 4. This table shows images of the particles of the raw materials used in the experiment, taken with a 200× Dino-Lite optical microscope, along with the sizes of the particles. In the modelling, recycle particles were chosen to be the maximum size of the experimental particles. The maximum value was selected because successful granulation of the wet mixture requires the diameter of the larger particles (in this case, the recycle) to be at least 1.5 times the diameter of the smaller particles (in this case, CU and MAChV).[50,51]

The granulation simulation of the mixture was carried out using single-sphere or dual-sphere particles. The recycle (60% of the total mass) was modelled using single-sphere particles with a diameter of 2.20 mm. This particle shape was selected because it most closely resembles the shape of the return granules used in the experiment.

Crystalline urea (36% of the total mass) was modelled using both single-sphere particles with a diameter of 1.50 mm and two-sphere particles with a diameter of 1.50 mm and a length of 2.25 mm. The single-sphere particles in the modelling represented urea crystals with a length-to-diameter ratio of approximately 1.00, while the two-sphere particles represented these crystals with a length-to-diameter ratio of approximately 1.50. Each type of particle represented half the mass of CU. Particle sizes were selected based on experimental results and estimated size ratios with recycle particles for the granulation simulation. MAChV (4% of the total mass) was modelled as single-sphere particles with a

Table 4 Geometry, mixture composition, flow rates and materials properties of experimental and DEM model particles

Properties	Materials/values: R	CU		MAChV
		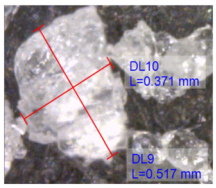	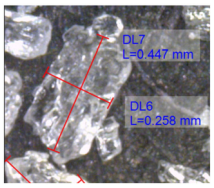	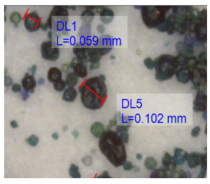
Experimental particle size,[a] mm	1.85 ± 0.35	1.10 ± 0.90	1.10 ± 0.90	0.33 ± 0.27
Experimental particle size range, mm	1.50–2.20	0.20–2.00	0.20–2.00	0.06–0.60
Percentage by weight	60%	18%	18%	4%
Shape of particle model	Single sphere	Single sphere	Dual sphere	Single sphere
Diameter of particle model, mm	2.20	1.50	1.50	0.90
Mass, g	30	9	9	2
Mass flow rate, g s^{-1}	1.00	0.60	0.60	0.07
Density, kg m^{-3}	1400			1100
Young's modulus, MPa	620			380
Poisson's ratio	0.25			

[a] Values represent mean ± standard deviation (n = 6).

Open Access Article. Published on 04 November 2025. Downloaded on 1/20/2026 7:39:08 PM.
This article is licensed under a Creative Commons Attribution 3.0 Unported Licence.

0.90 mm diameter. The single-sphere particles were modelled to have the same shape as microalgae. For the simulations, the particle size of the microalgae was chosen to be about 10 times larger. Microalgae, as a minor component, were modelled with particles ten times larger, following similar studies of finely dispersed powder mixture granulation.[48–51] To compensate for the modified geometric properties of the particles, the interparticle interactions were adjusted to achieve a simulated behaviour that closely matches experimental observations.

Literature surveys report the material density of CU to range from 1200 to 1400 kg m^{-3}. In the present modelling studies, a material density of 1400 kg m^{-3} was selected.[52] The primary component of the recycle material used in these studies was crystalline urea; consequently, the density of the recycle material was assumed to be equivalent to that of CU. Because data on the material density of MAChV are not available in the literature, it was assumed to be lower than that of CU, and a value of 1100 kg m^{-3} was selected.

Another important material property for accurate DEM modelling is Young's modulus. Literature reports on Young's modulus for CU exhibit a considerable range, typically between 250 and 800 MPa; for the present modelling studies, a Young's modulus of 620 MPa was adopted.[52] Given that recycle was granulated from urea, its Young's modulus was assumed to be identical to that of crystalline urea. Because data on MAChV elastic modulus are not available in the literature, it was assumed to be lower than that of crystalline urea. A value of 380 MPa was adopted for the elastic modulus of microalgae. The elastic modulus of paracetamol powder, a material with similar properties, was found to be comparable to the selected value for microalgae.[53]

The Poisson's ratio of crystalline urea typically falls within the range of 0.25 to 0.30. For the present modelling studies, a value of 0.25 was selected.[52] Given the relatively minor impact of Poisson's ratio compared to material density and Young's modulus in DEM modelling, identical values were adopted for all materials. In the modelling studies, the granulator was fed with a total mixture of 50 g for 30 seconds. After this initial feed, the entire mixture continued to be granulated and mixed within the granulator until the process was complete. The selected set of model particle properties resulted in simulations that agreed well with the experimental data, as shown in Fig. 7. This validation confirms the accuracy of the model in representing the granulation process.

3.3. Interactional properties of the particles

Granulation is primarily influenced by the particle–particle and particle–equipment static and dynamic friction coefficients,[54] coefficient of restitution, and the adhesive and cohesive properties of the particles.[53] These particle interaction properties are summarized in Table 5.

The particle–particle coefficient of restitution for crystalline urea was 0.22.[52] This value was used in the granulation modelling studies for urea and recycle, while a lower value of 0.18 was chosen for microalgae, as the literature lacks information on the coefficient of interaction for this material. The lower value of this coefficient was selected because microalgae is a softer material than crystalline urea, and the lower the value of the interaction coefficient, the softer the material. The associated particle properties are reported in ref. 48 and 50.

The coefficient of restitution between urea particles and the stainless-steel equipment contact surface was 0.55.[52] In the studies, the value of this coefficient for crystalline urea was assumed to be less than half of the value 0.22, as this was used to evaluate the effect of the liquid binder on the behaviour of the whole granulation mixture.[53] For the other material, recycle, these properties were assumed to be the same as those for urea, while a lower value was chosen for the coefficient of interaction for MAChV. The interaction coefficients between particles with similar properties and steel were determined to be 0.20 in ref. 48 and 50.

The particle–particle static friction coefficient for crystalline urea and particles with similar properties can range from 0.30 to 0.60.[48,50,52] As can be seen from Table 5 above, the particle–particle static friction coefficient for urea was set to the maximum value of 0.60. A higher value for this coefficient was chosen to account for the influence of the liquid binder on the overall mixture behaviour. Particles with a higher coefficient of static friction are more resistant to separation during wet granulation of the mixture. The value of this coefficient was chosen to be identical for recycle and microalgae.

The coefficient of particle–equipment static friction between CU or particles with similar properties and a stainless-steel surface can range from 0.30 to 0.70.[48,50,52] For

Table 5 Interaction properties of the particle models

	Materials/values					
	Recycle		CU		MAChV	
Interaction	Particle–particle	Particle–equipment	Particle–particle	Particle–equipment	Particle–particle	Particle–equipment
Coefficient of restitution	0.22	0.22	0.22	0.22	0.18	0.18
Coefficient of static friction	0.60	0.55	0.60	0.55	0.60	0.60
Coefficient of rolling friction	0.16	0.10	0.16	0.10	0.16	0.10
Surface energy, J m^{-2}	2.50	0.50	2.50	0.50	2.80	0.50

 This journal is © The Royal Society of Chemistry and IChemE 2026

Open Access Article. Published on 04 November 2025. Downloaded on 1/20/2026 7:39:08 PM.
This article is licensed under a Creative Commons Attribution 3.0 Unported Licence.

crystalline urea and recycle, a static friction coefficient of 0.55 was used, while for MAChV, a value of 0.60 was selected. The higher value of this coefficient was chosen due to its correlation with particle adhesion to the drum granulator walls.

The particle–particle coefficient of rolling friction for urea or very similar materials can range from 0.10 to 0.20.[48,50,52] The same value of 0.16 for this particle–particle rolling friction coefficient was chosen for all materials in these studies. To assess the impact of the liquid binder on particle adhesion to the granulator wall, the particle–equipment rolling friction coefficient was set to 0.10 for all materials. A higher value for the particle–equipment rolling friction coefficient was selected because the particles exhibited a greater tendency to adhere to one another than to the drum granulator walls during the experiments.

Due to the cohesive and adhesive nature of the mixture, the Hertz–Mindlin with JKR contact model was used to represent the contact behaviour between elastic particles in the simulation. Because it only requires one additional parameter: the interface energy – this contact model is well-suited for simulating the granulation of wet mixtures composed of finely dispersed particles with similar properties, such as iron ore and detergent powder.[53] Cohesion and adhesion between particles and surfaces are essential parameters in the granulation process, as they contribute to the formation of liquid–particle bridges and the seeding of smaller particles onto larger ones.[54,55] The surface adhesion energy for wet calcium carbonate powder in drum granulation was determined to be between 0.5 and 5.0 J m^{-2} using the Hertz–Mindlin with JKR contact model.[50]

To calibrate the interface energy properties of these particles, modelling studies were performed using the following surface energy values: 0.5, 1.5, 2.5, 3.5, and 4.5 J m^{-2}. The calibration tests assessed three parameters: the passage of the wet mixture through the hopper opening, the mixture's behaviour in the drum granulator, and the mixture's segregation coefficient value. A visual analysis of the simulated and experimental wet mixture flow and granulation processes indicated that the properties of the simulated mixture were most accurately represented when the particle–particle surface energy was 2.5 J m^{-2} and the particle–equipment surface energy was 0.5 J m^{-2}. The interface energy values indicate that the particles of the wet mixture exhibit greater interparticle adhesion but reduced adhesion to the walls, spiral, and blades of the drum granulator. During the granulation phase, the mixture adheres to the drum walls, but at a certain height, a fragment of the granulated mixture detaches and falls, leading to a complex process of mixing and granulation (Fig. 7).

3.4. Particle's total mass, total number of contacts and segregation

The generated particle mass as a function of time is shown in Fig. 4 below. The required total mass of 50 g of particles

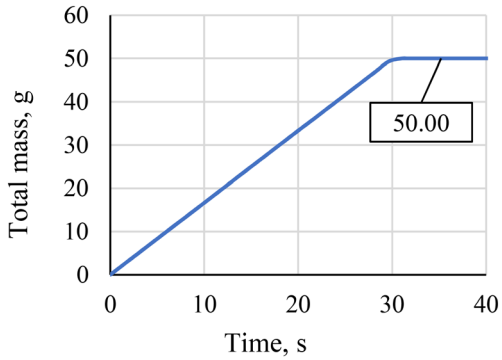

Fig. 4 Total mass of generated particles.

was produced in 25 seconds. However, when the total mass sensor was placed at a certain distance from the particle flow generation factory, the final accumulated mass of the particles was achieved in 30 seconds from the start. Once the required mass of particles was produced and loaded into the granulator, the mixing and granulation process began. The resulting particle flow is illustrated in Fig. 7. In the experimental study, a mixture of the raw materials and a liquid binder was granulated. The liquid binder is generally not modelled individually in DEM simulations, and its impact on the granulation of the raw material mixture is assessed by modifying the properties of the materials and their interactions.[49,53] The mass and segregation sensors in the modelling software were used to estimate the mass of the generated particles and the segregation of the granulated mixture. In the simulation of granulation of a fertilizer mixture, no granules are produced in the final stage of the granulation process, as opposed to the experiment.[50] Granulation is considered successful when smaller particles adhere to larger particles, resulting in a reduced number of contacts between individual particles.

The following Fig. 5 shows the time dependence of the number of particle contacts for the mixing and granulation processes. This dependence is an indication of the total amount of contacts that the particles have with each other and with the surface of the equipment. The total number of contacts increased significantly within the first 30 seconds

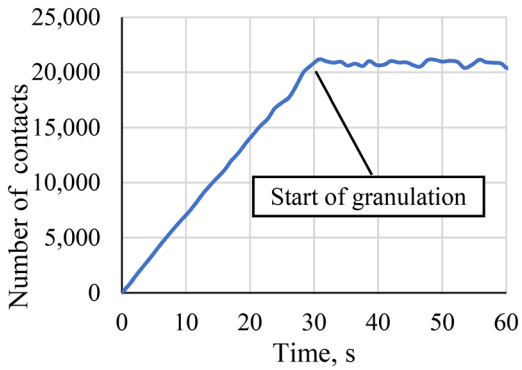

Fig. 5 Total number of contacts between large and fine particles during the granulation.

Open Access Article. Published on 04 November 2025. Downloaded on 1/20/2026 7:39:08 PM.
This article is licensed under a Creative Commons Attribution 3.0 Unported Licence.

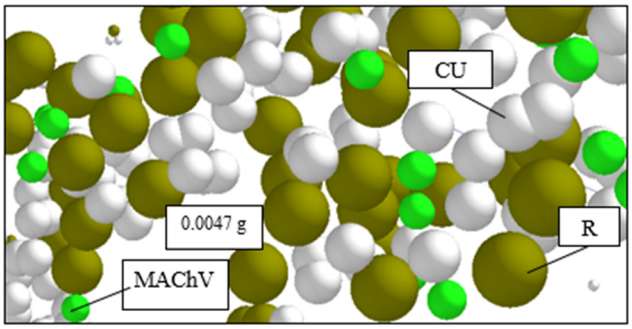

Fig. 6 Particle segregation value (0.0047 g) after 82.6 seconds of granulation.

due to the introduction of mixture particles into the granulator; however, this trend stabilized, forming a plateau. This is characterized by the absence of significant fluctuations, which indicates that the particles' relative positions remained consistent due to their stickiness. The particles began to adhere to each other, and granules started to form. In this case, granulation is considered to have been initiated approximately 30 seconds after modelling had begun.

Another parameter which indicates the quality of the granulated mixture is the degree of segregation. The degree of segregation, a critical parameter for evaluating the quality of the granulated mixture, was quantified using a virtual segregation sensor. The analysis involved continuously tracking the spatial distribution of a specific material (*e.g.*, MAChV) within the granular mixture throughout the simulation. The segregation value was then estimated by summing the total mass of the designated material that had migrated from its initial uniform distribution at a specified time. Fig. 6 shows a snapshot of the granulated particles in the granulator. For clarity, the granulator is not shown, and only the mixture particles are displayed. As can be seen from the presented figure, the resulting segregation value of the mixture was found to be 0.0047 g. This value, being exceptionally close to zero, indicates minimal particle segregation, which confirms the effectiveness of the granulation process. These results were recorded for up to 82.6 seconds, with a stable segregation value observed and negligible variation thereafter.

In the presented visualizations, a consistent colour scheme is used to differentiate particle types within the granular mixture. Green particles represent the MAChV, army khaki particles denote the R, and white particles correspond to the CU, including both single spheres and dual spheres. This scheme is applied uniformly throughout all the presented results of the simulation.

3.5. Formation of granules

Fig. 7 shows an image of the feeder and granulator with a mass of particles of granular material. For visual clarity, the hopper is shown as a solid object, and the granulator is shown as a transparent object.

The virtual "particle factory" is also shown positioned in the upper part of the hopper. The particle mixture was granulated, further granulated, and then gradually fed into

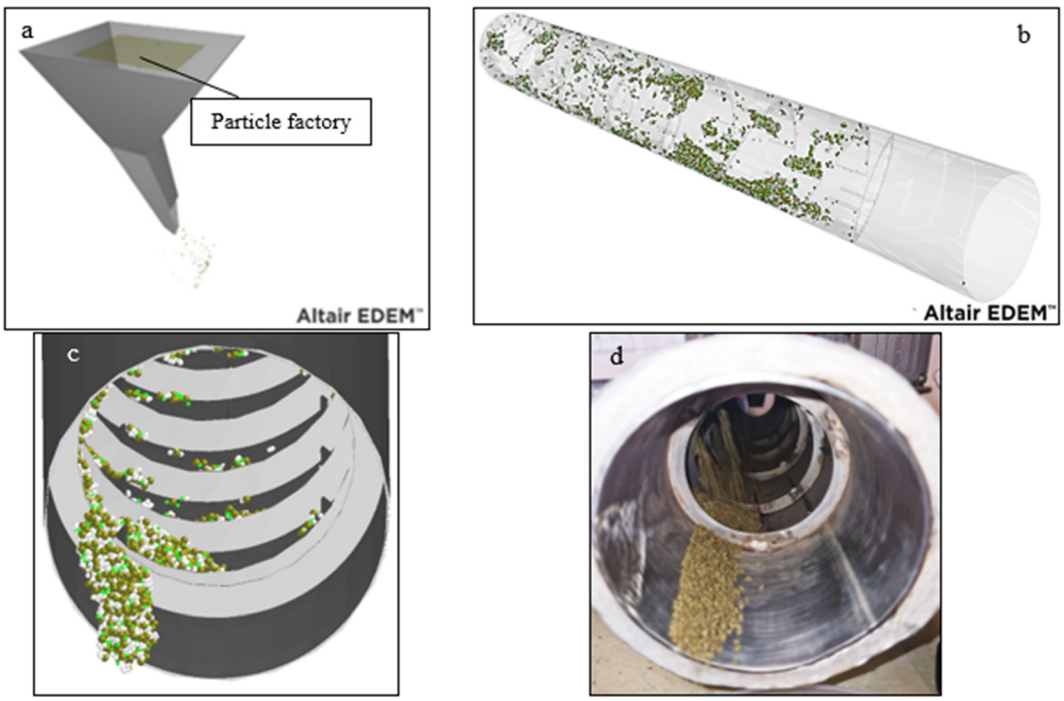

Fig. 7 A view of the granulator and the granulated particles: a) view of the hopper inlet, b) view along the granulator in modelling, c) view from the end of the granulator during modelling, and d) view from the end of the granulator during experiment.

 This journal is © The Royal Society of Chemistry and IChemE 2026

Open Access Article. Published on 04 November 2025. Downloaded on 1/20/2026 7:39:08 PM.
This article is licensed under a Creative Commons Attribution 3.0 Unported Licence.

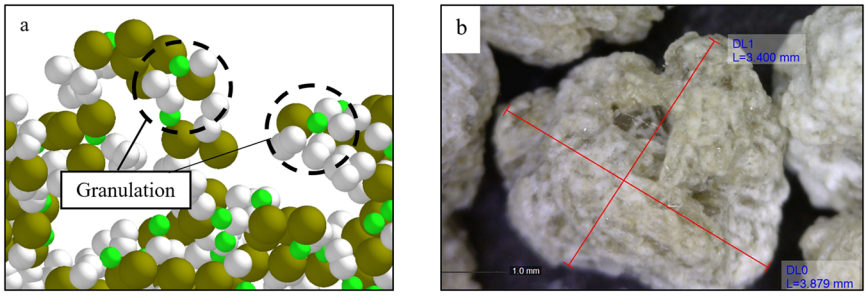

Fig. 8 Image: a) of the granule formed in simulation, b) of the granule from experiments. Green particles represent MAChV, army khaki particles show R, and white particles are CU.

the discharge section of the granulator. From the figures above, the behaviour of the granulating mixture in the simulation and experimental studies was quite similar. The mixture is lifted by the spiral and blades, and at a certain point, it drops down and continues to flow through the granulator in this mixing process.

Fig. 8 shows an image of the simulated granule, where the larger recycle particle is covered by smaller crystalline urea and microalgae particles. An optical microscope image at 60× magnification of the experimental granule is shown on the right.

As seen from the simulation results, the discrete element method can be used to carry out granulation studies on finely dispersed particles using a drum granulator.[55] To enhance model accuracy, further research on the properties of the granulation mixture is needed to calibrate particle characteristics, interaction properties, and parameters of surface energy.

The DEM model demonstrates high reliability within the calibrated and validated operating conditions. These include a drum rotation speed of 26 rpm, a drum inclination angle of 3°, a low fill level of about 2.8% of total volume, moderate raw material moisture content (~14%), and near-spherical particles with a seeded size distribution. The model also reflects the dynamics of the tested granulator geometry, including its length-to-diameter ratio and internal spiral and blade configuration. Readers should exercise caution when applying the model to conditions outside these limits. In particular, extreme moisture levels, strongly non-spherical particles, very different drum speeds or angles, alternative geometries, higher fill levels, or scale-up to industrial drums require recalibration and validation of the contact parameters. For practical use, we recommend starting within the tested operating window, as granule size, uniformity, and strength are most predictable under these conditions. This provides a reliable basis for process design and further optimization.

4. Conclusions

This study shows that DEM can successfully simulate the wet granulation of a microalgae-enriched nitrogen fertilizer mixture. The new contribution of this work is a predictive DEM model that captures essential stages of granule formation and supports the optimization of fertilizer production parameters.

Adding recycle to the raw mixture significantly influences granule size distribution. Specifically, with 20% and 40% recycle additions, there is a notable increase in the amounts of granules of size between 1.0–2 mm and 2.0–3.15 mm compared to granulation without recycle. Notably, at a 60% recycle addition, the fraction of commercial granules (sized 2.0–4.0 mm) yields approximately 68%. This result suggests that the percentage of recycle directly influences the formation of granules within the desired size ranges.

Granules produced with higher amounts of recycle exhibit lower static strength. This reduction is most likely attributable to a less uniform particle size distribution, weaker interaction forces between particles of varying sizes, a diminished elastic–plastic effect, and poorer agglomeration.

The granulation of a mixture comprising recycle, crystalline urea, and finely dispersed microalgae was simulated using a model of an actual experimental granulation drum. Particles of materials were modelled as single-sphere and dual-sphere particles, with shapes and sizes approximating those of the experimental materials.

Experiments were conducted using a wet granulation process with a binder. To assess the influence of the liquid binder on the mixture behaviour during granulation simulation, particle–particle, particle–equipment, and adhesion–cohesion properties within the model were modified. These adjusted properties were calibrated through simulations and demonstrated reasonable agreement with experimental results.

Simulations indicated that the target quantity of the granulation mixture was produced within 30 seconds, while granulation for the studied materials commenced after approximately 30 seconds. Throughout the granulation process, the segregation coefficient of the model mixture remained near zero, and granule formation began in the granulation and discharge sections of the granulator.

For the granular fertilizer production industry, this study represents a significant advancement in understanding the process and optimizing it. The detailed quantitative and qualitative evaluation of the granulation effect was not included due to the considerable complexity and inherent

Open Access Article. Published on 04 November 2025. Downloaded on 1/20/2026 7:39:08 PM.
This article is licensed under a Creative Commons Attribution 3.0 Unported Licence.

challenges associated with the selection and calibration of numerous microscopic contact model parameters within the discrete element method (DEM). However, current findings already provide a foundational understanding of the granulation mechanism of microalgae-enriched urea fertilizers. A broader parametric study conducted by us or other researchers in the future can provide deeper insights into the optimal operating conditions and material properties.

Conflicts of interest

There are no conflicts to declare.

Data availability

The data that support the findings of this study are available from the corresponding author upon reasonable request.

These are scientific experimental data of PhD student Austėja Mikolaitienė (supervisor dr. Rasa Šlinkšienė), which have not been previously published and were presented during the dissertation defence on 2025-06-13 at Kaunas University of Technology.

References

1 Sod Solutions, Granular *vs.* Liquid fertilizers, 2023, https://sodsolutions.com/lawn-garden-nutrition/granular-vs-liquid-fertilizers/, (accessed on 1 October 2024).
2 Nutri Norm powered by OCI, Physical properties of granular fertilisers, 2023, https://nutrinorm.co.uk/spreading/spreading-fertilisers/physical-properties-of-granular-fertilisers/, (accessed on 1 October 2024).
3 M. E. Trenkel, Slow-and controlled-release and stabilized fertilizers: an option for enhancing nutrient use efficiency in agriculture, International Fertilizer Association (IFA), Paris, 2010.
4 B. Azeem, K. KuShaari and Z. B. Man, *et al.*, Review on materials & methods to produce controlled release coated urea fertilizer, *J. Controlled Release*, 2014, **181**, 11–21, DOI: 10.1016/j.jconrel.2014.02.020.
5 R. Rose, Slow release fertilizers 101, in *Technical*, ed. R. K. Dumroese, L. E. Riley and T. D. Landis, 2002, https://research.fs.usda.gov/treesearch/31411.
6 U. Akira, K. Kihachiro and S. Tadami, Patent publication JPH0230690A, China, 1990.
7 M. K. Yusop, F. Mahdavi and S. A. Rashid, *et al.*, Enhancement of nitrogen release properties of urea–kaolinite fertilizer with chitosan binder, *Chem. Speciation Bioavailability*, 2015, **27**(1), 44–51, DOI: 10.1080/09542299.2015.1023090.
8 Y. Ding, Y. X. Liu and W. X. Wu, *et al.*, Evaluation of Biochar Effects on Nitrogen Retention and Leaching in Multi-Layered Soil Columns, *Water, Air, Soil Pollut.*, 2010, **213**(1), 47–55, DOI: 10.1007/s11270-010-0366-4.
9 T. Pursell, A. R. Shirley Jr. and K. D. Cochran, *et al.*, Controlled release fertilizer with biopolymer coating and process for making same, *US Pat.*, US20120090366A1, 2012.
10 M. I. Khan, J. H. Shin and J. D. Kim, The promising future of microalgae: current status, challenges, and optimization of a sustainable and renewable industry for biofuels, feed, and other products, *Microb. Cell Fact.*, 2018, **17**, 36, DOI: 10.1186/s12934-018-0879-x.
11 P. Baweja, S. Kumar and G. Kumar, Organic Fertilizer from Algae: A Novel Approach Towards Sustainable Agriculture, *Biofertilizers for Sustainable Agriculture and Environment*, 2019, vol. 1, pp. 353–370, DOI: 10.1007/978-3-030-18933-4_16.
12 A. R. Lewin and R. A. Andersen, Algae, *Encyclopedia Britannica*, https://www.britannica.com/science/algae, (accessed 25 October 2024).
13 A. Vidyasagar, What Are Algae?, LiveScience, 2016, https://www.livescience.com/54979-what-are-algae.htm, (accessed 25 October 2024).
14 C. G. Vassilev and S. V. Vassilev, Composition, Properties and Challenges of Algae Biomass for Biofuel Application: An Overview, *Fuel*, 2016, **181**, 1–33, DOI: 10.1016/j.fuel.2016.04.106.
15 A. Demibras, Biofuels Production from Microalgae by Liquefaction and Supercritical Water Pyrolysis, *Energy Sources, Part A*, 2017, **39**(8), 827–834, DOI: 10.1080/15567036.2016.1269143.
16 J. S. Chang, W. H. Chen and K. L. Yu, *et al.*, Show, Microalgae from Wastewater Treatment to Biochar – Feedstock Preparation and Conversion Technologies, *Energy Convers. Manage.*, 2017, **150**, 1–13, DOI: 10.1016/j.enconman.2017.07.060.
17 K. Dhirendra and N. Kumar, Effect of FYM, NPK and Algal Fertilizers on the Growth and Biomass of Vetiver Grass [Vetiveria zizanioides L.Nass], *Int. J. Eng. Appl. Sci.*, 2016, **3**(3), 85–89, https://www.ijeas.org/effect-of-fym-npk-and-algal-fertilizers-on-the-growth-and-biomass-of-vetiver-grass-vetiveria-zizanioides-lnass.
18 P. Sumran, B. Sunun and K. Thawan, Application of Blue-Green Algae and Mineral Fertilizers to Direct Seeding Lowland Rice, *ScienceAsia*, 2015, **41**, 305–314, DOI: 10.2306/scienceasia1513-1874.2015.41.305.
19 A. M. Sánchez Mirón, C. Cerón Garcıa and A. Contreras Gómeza, *et al.*, Shear stress tolerance and biochemical characterization of Phaeodactylum tricornutum in quasi steady-state continuous culture in outdoor photobioreactors, *Biochem. Eng. J.*, 2003, **16**(3), 287–297, DOI: 10.1016/S1369-703X(03)00072-X.
20 C. Posten, Design principles of photo-bioreactors for cultivation of microalgae, *Eng. Life Sci.*, 2009, **9**(3), 165–177, DOI: 10.1002/elsc.200900003.
21 B. Zhao, Y. Zhang and K. Xiong, *et al.*, Effect of cultivation mode on microalgal growth and CO_2 Fixation, *Chem. Eng. Res. Des.*, 2017, **89**(9), 1758–1762, DOI: 10.1016/j.cherd.2011.02.018.
22 T. M. Mata, A. A. Martins and N. S. Caetano, Microalgae for biodiesel production and other applications: A review, *Renewable Sustainable Energy Rev.*, 2010, **14**(1), 217–232, DOI: 10.1016/j.rser.2009.07.020.

 This journal is © The Royal Society of Chemistry and IChemE 2026

Open Access Article. Published on 04 November 2025. Downloaded on 1/20/2026 7:39:08 PM.
This article is licensed under a Creative Commons Attribution 3.0 Unported Licence.

23 T. T. Y. Doan, B. Sivaloganathan and J. P. Obbard, Screening of marine microalgae for biodiesel feedstock, *Biomass Bioenergy*, 2011, **35**(7), 2534–2544, DOI: 10.1016/j.biombioe.2011.02.021.
24 C. Yoo, S. Y. Jun and J. Y. Lee, *et al.*, Selection of microalgae for lipid production under high levels carbon dioxide, *Bioresour. Technol.*, 2010, **101**(1), 71–74, DOI: 10.1016/j.biortech.2009.03.030.
25 C. Yeesang and B. Cheirsilp, Effect of nitrogen, salt, and iron content in the growth medium and light intensity on lipid production by microalgae isolated from freshwater sources in Thailand, *Bioresour. Technol.*, 2011, **102**(3), 3034–3040, DOI: 10.1016/j.biortech.2010.10.013.
26 R. Kumari, I. Kaur and A. K. Bhatnagar, Effect of aqueous extract of Sargassum johnstonii Setchell & Gardner on growth, yield and quality of Lycopersicon esculentum Mill, *J. Appl. Phycol.*, 2011, **23**, 623–633, DOI: 10.1007/s10811-011-9651-x.
27 J. Coppens, O. Grunert and S. Van Den Hende, The use of microalgae as a high-value organic slow-release fertilizer results in tomatoes with increased carotenoid and sugar levels, *J. Appl. Phycol.*, 2016, **28**, 2367–2377, DOI: 10.1007/s10811-015-0775-2.
28 E. R. Tarakhovskaya, Y. I. Maslov and M. Shisshova, Phytohormones in algae, *Russ. J. Plant Physiol.*, 2007, **54**(2), 163–170, DOI: 10.1134/S1021443707020021.
29 W. D. Temple and A. A. Bomke, Effects of kelp (*Macrocystis integrifolia*) on soil chemical properties and crop response, *Plant Soil*, 1988, **105**, 213–222, DOI: 10.1007/BF02376785.
30 W. Mulbry, E. K. Westhead, C. Pizarro and L. Sikora, Recycling of manure nutrients: use of algal biomass from dairy manure treatment as a slow release fertilizer, *Bioresour. Technol.*, 2005, **96**(4), 451–458, DOI: 10.1016/j.biortech.2004.05.026.
31 W. Mulbry, S. Kondrad and C. Pizarro, Biofertilizers from Algal Treatment of Dairy and Swine Manure Effluents, *J. Veg. Sci.*, 2017, **12**(4), 107–125, DOI: 10.1300/J484v12n04_08.
32 W. Gang, L. Changxin and L. Yongbo *et al.*, Chinese Patent CN110526761A, 2019.
33 C. Jiahui, Chinese Patent CN104211547A, 2014.
34 ISO 18645:2016(E), Fertilizers and soil conditioners – Water soluble fertilizer – General requirements, accessed on 1 October 2024, https://www.iso.org/obp/ui/en/#iso:std:iso:18645:ed-1:v1:en.
35 CEN REPORT, Fertilizers – Crushing strength determination on fertilizer grains, CEN/TR 12333:2021, https://standards.iteh.ai/catalog/standards/cen/a94a46ef-b1e0-4eda-b845-dd6c62c1ab5f/cen-tr-12333-2021?srsltid=AfmBOooktq7fwWGb1c0m_gFfnqJ6WV4Myq3KB6mJ6o5fhSHYaaOcBua1, (accessed on 25 November 2024).
36 EUROPEAN STANDARDS DIN EN 1236 Fertilizers - Determination of bulk density (loose) (ISO 3944:1992, modified), https://www.en-standard.eu/din-en-1236-fertilizers-determination-of-bulk-density-loose-iso-3944-1992-modified/, (accessed on 25 November 2024).
37 M. F. McGuire, *Stainless steels for design engineers*, Asm International, Materials Park, OH, 2008.
38 A. Mikolaitienė and R. Šlinkšienė, Effect of Various Binders on the Properties of Microalgae-Enriched Urea Granules, *Plants*, 2022, **11**(23), 3362, DOI: 10.3390/plants11233362.
39 K. Jančaitienė and R. Šlinkšienė, Influence of cellulose additive on the granulation process of potassium dihydrogen phosphate, *Chem. Ind. Chem. Eng. Q.*, 2020, **26**(4), 359–367, DOI: 10.2298/CICEQ191029013J.
40 R. Šlinkšienė, E. Sendzikienė and A. Mikolaitienė, *et al.*, Use of microalgae biomass for production of granular nitrogen biofertilizers, *Green Chem. Lett. Rev.*, 2022, **15**(2), 416–426, DOI: 10.1080/17518253.2022.2071593.
41 D. Ragauskaitė and R. Šlinkšienė, Influence of urea on organic bulk fertilizer of spent coffee grounds and green algae Chlorella sp. biomass, *Sustainability*, 2022, **14**(3), 1261, DOI: 10.3390/su14031261.
42 O. Pocienė and R. Šlinkšienė, Properties and production assumptions of organic biofertilisers based on solid and liquid waste from the food industry, *Appl. Sci.*, 2024, **14**(21), 9784, DOI: 10.3390/app14219784.
43 N. Woodroof, Size Matters, World Fertilizer, 2021, https://www.worldfertilizer.com/special-reports/05042021/size-matters, (accessed 25 October 2024).
44 M. Xin, Z. Jiang and Y. Song, *et al.*, Compression Strength and Critical Impact Speed of Typical Fertilizer Grains, *Agriculture*, 2023, **13**, 2285, DOI: 10.3390/agriculture13122285.
45 FerTech Inform, The two main granulation processes, 2022, https://fertechinform.org/knowledgebase/the-two-main-granulation-processes/, (accessed 25 October 2024).
46 M. Przywara, R. Dürr and E. Otto, *et al.*, Process Behavior and Product Quality in Fertilizer Manufacturing Using Continuous Hopper Transfer Pan Granulation – Experimental Investigations, *Processes*, 2021, **9**, 1439, DOI: 10.3390/pr9081439.
47 M. Macák and K. Krištof, The effect of granulometric structure and moisture of fertilizer on its static strength, *Res. Agric. Eng.*, 2016, **62**(10), S1–S7, DOI: 10.17221/31/2016-RAE.
48 A. Hassanpour, M. Pasha and L. Susana, *et al.*, Analysis of seeded granulation in high shear granulators by discrete element method, *Powder Technol.*, 2013, **238**, 50–55, DOI: 10.1016/j.powtec.2012.06.028.
49 Y. You, J. Guo and G. Li, *et al.*, Investigation the iron ore fine granulation effects and particle adhesion behavior in a horizontal high-shear granulator, *Powder Technol.*, 2021, **394**, 162–170, DOI: 10.1016/j.powtec.2021.08.047.
50 M. A. Behjani, N. Rahmanian, N. F. b. A. Ghani and A. Hassanpour, An investigation on process of seeded granulation in a continuous drum granulator using DEM, *Adv. Powder Technol.*, 2017, **28**(10), 2456–2464, DOI: 10.1016/j.apt.2017.02.011.
51 P. Roy, M. Vashishtha, R. Khanna and D. Subbarao, Variation of granule mass fraction with coordination number in wet granulation process, *Particuology*, 2009, **7**(5), 408–413, DOI: 10.1016/j.partic.2009.07.001.

Open Access Article. Published on 04 November 2025. Downloaded on 1/20/2026 7:39:08 PM.
This article is licensed under a Creative Commons Attribution 3.0 Unported Licence.

52 S. A. Nouh, K. KuShaari, L. K. Keong and S. Samsuri, Material characterization and inter/intra-particle validation for DEM simulation of urea coating process, *Particuology*, 2024, **88**, 32–48, DOI: 10.1016/j.partic.2023.09.010.

53 J. P. Morrissey, K. J. Hanley and J. Y. Ooi, Conceptualisation of an Efficient Particle-Based Simulation of a Twin-Screw Granulator, *Pharmaceutics*, 2021, **13**(12), 2136, DOI: 10.3390/pharmaceutics13122136.

54 H. Nakamura, T. Baba and S. Ohsaki, *et al.*, Numerical simulation of wet granulation using the DEM–PBM coupling method with a deterministically calculated agglomeration kernel, *Chem. Eng. J.*, 2022, **450**, 138298, DOI: 10.1016/j.cej.2022.138298.

55 T. Baba, H. Nakamura and H. Takimoto, *et al.*, DEM–PBM coupling method for the layering granulation of iron ore, *Powder Technol.*, 2021, **378**, 40–50, DOI: 10.1016/j.powtec.2020.09.059.

 This journal is © The Royal Society of Chemistry and IChemE 2026